Developmental Cell
Article

Otx2 and Onecut1 Promote the Fates of Cone Photoreceptors and Horizontal Cells and Repress Rod Photoreceptors

Mark M. Emerson,[1,3] Natalia Surzenko,[1] Jillian J. Goetz,[2] Jeffrey Trimarchi,[2] and Constance L. Cepko[1,*]
[1]Departments of Genetics and Ophthalmology, Howard Hughes Medical Institute, Harvard Medical School, Boston, MA 02115, USA
[2]Department of Genetics, Development and Cell Biology, Iowa State University, Ames, IA 50011, USA
[3]Present address: Department of Biology, The City College of New York, City University of New York, New York, NY 10031, USA
*Correspondence: cepko@genetics.med.harvard.edu
http://dx.doi.org/10.1016/j.devcel.2013.06.005

SUMMARY

Cone photoreceptors carry out phototransduction in daylight conditions and provide the critical first step in color vision. Despite their importance, little is known about the developmental mechanisms involved in their generation, particularly how they are determined relative to rod photoreceptors, the cells that initiate vision in dim light. Here, we report the identification of a *cis*-regulatory module (CRM) for the thyroid hormone receptor beta (*Thrb*) gene, an early cone marker. We found that ThrbCRM1 is active in progenitor cells biased to the production of cones and an interneuronal cell type, the horizontal cell (HC). Molecular analysis of ThrbCRM1 revealed that it is combinatorially regulated by the Otx2 and Onecut1 transcription factors. Onecut1 is sufficient to induce cells with the earliest markers of cones and HCs. Conversely, interference with Onecut1 transcriptional activity leads to precocious rod development, suggesting that Onecut1 is critically important in defining cone versus rod fates.

INTRODUCTION

Vertebrate photoreceptor cells are a highly specialized class of cells that capture and process light, initiating the first steps in vision (Rodieck, 1998). The two classes of photoreceptors are rod photoreceptors (rods) and cone photoreceptors (cones). Rods respond to low light levels while cones subserve vision under daylight-luminance conditions. The importance of cones is underscored by the severe impairment of high-acuity vision that accompanies their loss in the course of several human retinal diseases, such as retinitis pigmentosa and macular degeneration (Gehrs et al., 2006; Hartong et al., 2006). Development of therapeutic approaches for these diseases includes the engraftment of photoreceptor cells generated by stem cells from various sources (Ong and da Cruz, 2012). The limited numbers of cone-photoreceptor-like cells generated in culture and their inefficient engraftment in the retina suggest that factors that can specifically increase the production of cones and endow them with the properties needed for integration and function in vivo would be useful (see West et al., 2012, for example).

The homeobox transcription factor Otx2 is a critical component in photoreceptor specification as it is expressed by all photoreceptors and necessary for their genesis (Nishida et al., 2003). However, Otx2 is also necessary for the development of horizontal cells (HCs) and bipolar cells within the retina (Koike et al., 2007; Nishida et al., 2003). Its role in HCs is particularly intriguing as Otx2 has not been observed in identifiable HCs, suggesting that it may act in a very early step in their development (Emerson and Cepko, 2011). Recent work has identified a *cis*-regulatory module (CRM) for the *Otx2* gene that is expressed in both early photoreceptors and early HCs, suggesting that there could be shared mechanisms involved in their genesis (Emerson and Cepko, 2011). In addition to Otx2, the transmembrane receptor Notch has been implicated as a critical negative regulator of photoreceptor development (Jadhav et al., 2006; Yaron et al., 2006). However, the identity of other factors that cooperate with Otx2 and Notch to establish photoreceptor cell fate is still unknown, though there is evidence that basic-helix-loop-helix (bHLH) genes function in rod specification (Cherry et al., 2011; Hatakeyama et al., 2001).

Rods and cones share the same basic function and specialized morphological features as well as gene expression. This could suggest that there are common mechanisms involved in their development. Several studies have pointed to the Maf family transcription factor neural retina leucine zipper gene (Nrl) as the critical determinant of rod versus cone photoreceptor fate (Daniele et al., 2005; Mears et al., 2001; Oh et al., 2007) (Figure 1). The current model of photoreceptor development posits that a postmitotic photoreceptor precursor cell is generated during development that can give rise to either a cone or a rod. This cell has the cone cell fate as its default, but if it expresses Nrl, it will become a rod (Swaroop et al., 2010) (Figure 1). However, the interpretation of these experiments has relied largely on changes in gene expression of mature photoreceptors. Thus, it is unclear whether Nrl regulates the fate choice of rod versus cone fate at the time of their genesis or whether it regulates rod- and cone-specific gene expression after an upstream determination event. Furthermore, the genetic programs that drive early cone gene expression are unknown.

Retinal cell types are generated from retinal progenitor cells (RPCs) in overlapping windows of developmental time. Retinal

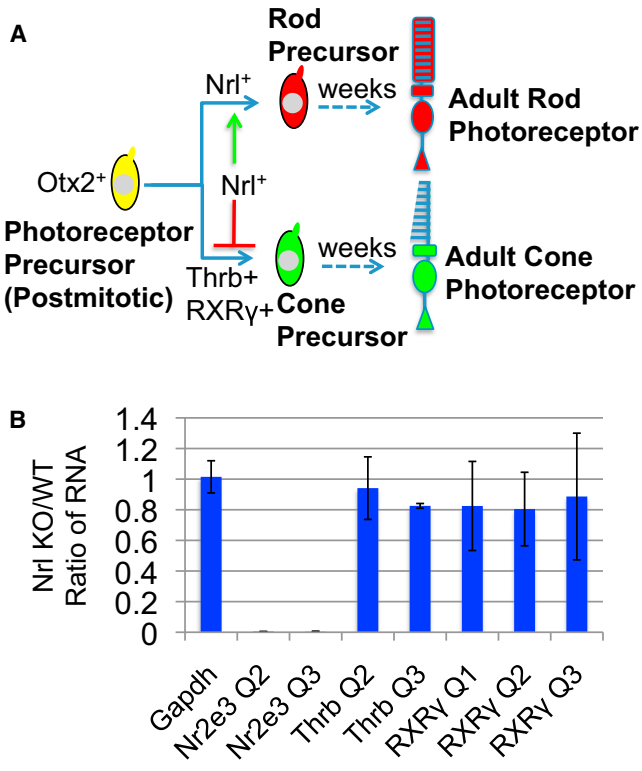

Figure 1. Examination of Photoreceptor mRNA Levels in Nrl Knockout Retinas

(A) A current model of photoreceptor specification (based on Swaroop et al., 2010).

(B) qPCR analysis of mRNA for rod and cone genes in retinal complementary DNA from P0 using the qPCR primer pairs for the gene noted along the x axis. The y axis represents the fold difference of relative RNA levels between WT and *Nrl* KO mice. Error bars represent SD.

ganglion cells, cones, and HCs are born almost exclusively in the embryonic retina and bipolar cells, and Mueller glia are born mainly in the postnatal period in mice and rats. Rod and amacrine cell genesis spans both the embryonic and postnatal periods (Sidman, 1961; Carter-Dawson and LaVail, 1979; Young, 1985). Early studies of lineage in the rodent retina using retroviral labeling demonstrated that many RPCs were multipotent and were able to produce overlapping combinations of cell types (Turner and Cepko, 1987; Turner et al., 1990). However, recent work has suggested that, at least in some cases, a terminal division of a specific type of RPC generates particular daughter cell types. We recently reported that in the mouse, we could direct retroviral infection to RPCs that expressed *Olig2*, a bHLH gene (Hafler et al., 2012). Infection of embryonic day 13.5 (E13.5) *Olig2*+ RPCs revealed that these RPCs are heavily biased to produce cones and HCs (referred to hereafter as an RPC[CH]), while in the postnatal period, the *Olig2*+ RPC population generated almost exclusively rods and amacrine cells (Hafler et al., 2012). Moreover, work in both chicken and fish have demonstrated the existence of an RPC that makes only HCs (Godinho et al., 2007; Rompani and Cepko, 2008). The molecular identity of the pathways that establish these restricted progenitor states is unknown.

In order to better understand the developmental origins of cones, we have investigated the transcriptional regulation of the *Thrb* gene, one of the earliest and most specific cone genes known to date (Ng et al., 2001, 2009). We identified the ThrbCRM1 element, which is active in RPCs that generate HCs and cones and is coregulated by the Otx2 and Onecut1 (OC1) transcription factors. These factors are coexpressed in a subset of embryonic RPCs. Misexpression of OC1 in the postnatal period is sufficient to induce the expression of early markers of both cones and HCs. Conversely, loss-of-function studies support a role for OC1 in promoting the cone fate at the expense of the rod fate and suggest that OC1 acts genetically upstream of *Nrl*. These studies identify key molecular components that establish the RPC[CH] state and identify OC1 as a critical determinant of cone versus rod identity.

RESULTS

Early Cone Photoreceptor Gene Expression Is Not Regulated by Nrl

The prevailing photoreceptor genesis model posits that a postmitotic cell is specified to become a photoreceptor by expression of Otx2, along with other unidentified factors (Figure 1A). Expression of the Maf family transcription Nrl in these cells is thought to suppress the program that results in the genesis of cones while promoting the rod fate (Swaroop et al., 2010). One foundation for this model is the observation that adult photoreceptors in *Nrl* knockout (KO) mice lack rod-specific markers and upregulate cone-specific ones (Daniele et al., 2005; Hsiau et al., 2007; Mears et al., 2001). However, it is unclear whether these photoreceptors are completely or partially transformed into cones and when this change occurs developmentally. To investigate these questions, we examined the expression of *Thrb* and *RXRγ* in the developing retina of Nrl KO mice. These two genes have been used to positively identify newborn cones and are thought to be absent in rods (Mori et al., 2001; Ng et al., 2001, 2009; Roberts et al., 2005). If *Nrl* is indeed the most upstream factor driving the photoreceptor precursor decision to become a rod, then these early cone genes should be upregulated in *Nrl* KO photoreceptors when rods are normally generated. Contrary to this prediction, quantitative PCR (qPCR) analysis revealed that both *Thrb* and *RXRγ* expression were unchanged in postnatal day (P) 0 Nrl KO retinas, a time when 50% of rods have been produced (Figure 1B) (Carter-Dawson and LaVail, 1979). This is in agreement with a previous study reporting wild-type *RXRγ* levels at P2 and only upregulated at P10 in the *Nrl* KO mouse, suggesting that *Nrl* is involved in later RXRγ regulation (Yoshida et al., 2004). In contrast, the Nrl target gene *Nr2e3* exhibited a dramatic reduction in expression in the *Nrl* KO, confirming that this is normally a time of active transcriptional regulation by Nrl (Figure 1B). These data suggest that additional factors regulate early cone gene expression independently of Nrl function.

Identification of Thrb *cis*-Regulatory Modules

To identify gene regulatory networks (GRNs) involved in cone genesis, CRMs responsible for *Thrb* expression were sought, as *Thrb* is the earliest, and most specific, known marker of cones (Ng et al., 2009). Phylogenetically conserved genomic elements

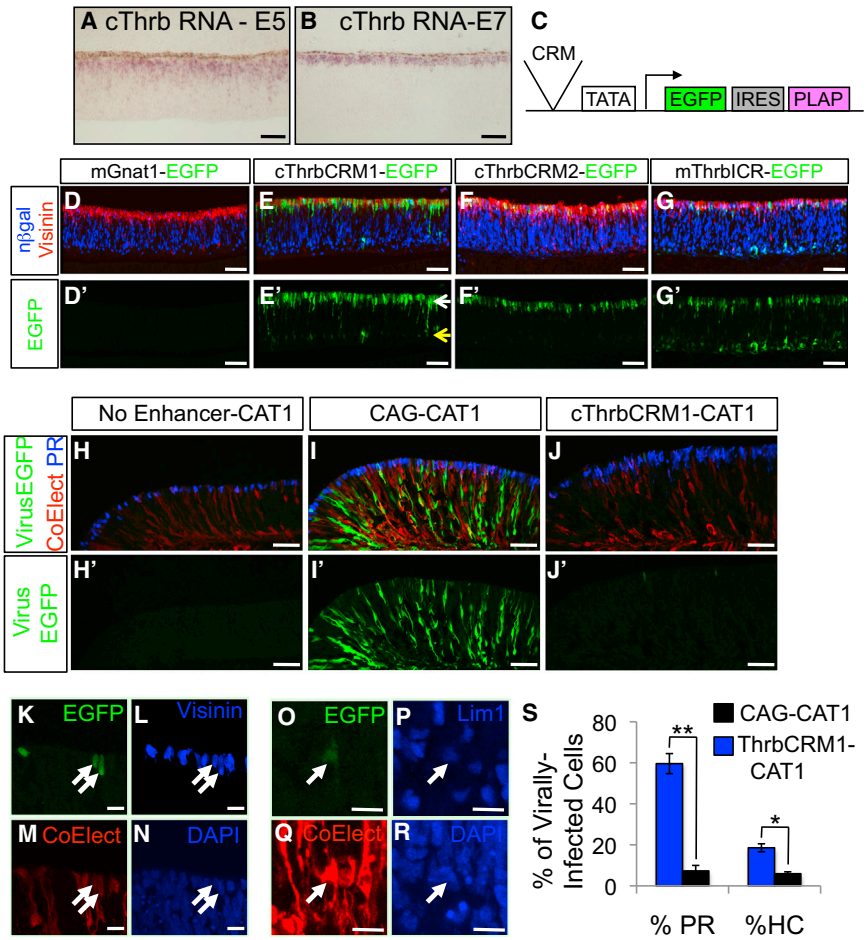

Figure 2. Identification and Analysis of Thrb CRMs

(A and B) RNA in situ hybridization for *cThrb* at E5 (A) and E7 (B) in central chicken retina.

(C) Schematic of the Stagia3 reporter vector.

(D–G) E5 retinas were coelectroporated with CAG-nβ-gal plasmids and Stagia3 plasmids, cultured for 2 days, sectioned, and immunohistochemically stained with αEGFP (green), αVisinin (red), and αβ-gal (blue). The electroporated Stagia3 reporter is shown above each column of images.

(D′–G′) EGFP channels alone of the above images. The white arrow in E′ shows the position of GFP+ cells just vitread to the scleral surface, and the yellow arrow shows the GFP+ cells just sclerad to the vitreal surface.

(H–J) Analysis of RPC progeny that express ThrbCRM1. Antigens detected were EGFP (green), AU1 (red), and Visinin (blue). The CAT1 plasmids used are shown at the top of each column.

(H′–J′) EGFP channels alone of the images in (H)–(J).

(K–R) Magnified views of ThrbCRM1-CAT1 retinas detected for viral EGFP (K and O), Visinin (L), AU1 (coelectroporation control) (M and Q), DAPI (N and R), and Lim1 (P).

(S) Percentage of virally transduced EGFP-positive cells that were identified as photoreceptors (Visinin+) or HCs (Lim1+) in retinas with the ThrbCRM1-CAT1 (blue bars) or CAG-CAT1 elements (black bars). Values represent the average of the data from three biological replicates. Error bars represent SEM. A two-tailed t test was used to assess statistical significance (**$p < 0.001$; *$p < 0.005$).

Scale bar represents 40 μm for (A), (B), (D)–(G), (D′)–(G′), (H)–(J), and (H)′–(J′) and 10 μm for (K–R). See also Figures S1 and S2.

in proximity to the *Thrb* locus were identified and tested for their ability to drive reporter gene expression in a *Thrb*-like pattern (Figures 2A–2C; Figure S1A available online). In E5 central chick retina, *cThrb* is found predominantly in the upper third of the retina, while *cThrb* is found in a more compact layer of cells by E7 (Figures 2A and 2B). Reporter constructs were tested in the chicken retina by ex vivo electroporation because of the large number of cones in the chick as well as our previous work showing that it was a robust system for CRM identification in the retina (Emerson and Cepko, 2011). At 2 days after DNA introduction, the retinas electroporated with a control mGnat1CRM plasmid that would not be expected to be active had no EGFP expression (Figures 2D and 2D′). In contrast, ThrbCRM1 drove reporter expression in newborn photoreceptors (Visinin+ cells) as well as two other populations of cells and was active within 6 hr of electroporation (Figures 2E and 2E′; data not shown) (Fischer et al., 2008). ThrbCRM2 was active in Visinin-positive cells but not the other two populations marked by ThrbCRM1 reporter activity, and it was not active at 24 hr postelectroporation (Figures 2F and 2F′; data not shown). Previously, a CRM referred to as a Thrb intron control region (ThrbICR) was characterized using transgenic mice (Jones et al., 2007). When tested in our assay, the intron control region was active in Visinin-positive photoreceptors as well as a number of other cells (Figures 2G and 2G′). Both ThrbCRM1 and ThrbICR had similar reporter activity 6 hr after electroporation (data not shown). These two elements could be active in the same set of cells, perhaps even sharing a GRN. To determine if this was a possibility, coelectroportation of two plasmids encoding the two elements upstream of unique reporters was introduced into the chicken retina. A large number of cells coexpressed the two reporters, suggesting that these two elements could share a GRN (data not shown).

Sequence Elements of ThrbCRM1 and Activity Restricted to the Period of Cone Genesis

To determine the critical sequence elements of ThrbCRM1, alignments of the homologous sequences among diverse vertebrate species were generated for the ThrbCRM1 element and the ThrbICR (Figures S1B and S1C). The most extensive conservation in ThrbCRM1 included an 8 bp stretch of nucleotides that was conserved in all of the species examined, and the same exact sequence was found to be present and conserved in the ThrbICR element (Figures S1B and S1C). Mutations in the 8 bp element of ThrbCRM1 and ThrbICR produced a large decrease in reporter expression in E5 chicken retinas (data not shown). We tested whether 40 bp fragments encompassing this sequence were sufficient to recapitulate the ThrbCRM1 activity. Two copies of the 40 bp element drove reporter activity above

background levels and closely matched that of the original element, as did four copies (all further experiments using ThrbCRM1 were performed with this 4 × 40 bp construct unless otherwise noted) (Figures S1B, S1D, S1D′, S1E, and S1E′). Mutations that changed the sequence in the 8 bp element dramatically decreased the activity of the 40 bp element (Figures S1F and S1F′).

The localized GFP reporter expression pattern driven by ThrbCRM1 was qualitatively very similar to the *cThrb* RNA expression pattern. To quantify this overlap, chicken E5 retinas were electroporated ex vivo with the ThrbCRM1-GFP reporter and a CAG-nβ-gal plasmid to detect the electroporated cells. After 8 hr of culture, retinas were dissociated into single cells and processed to detect endogenous *cThrb* messenger RNA (mRNA) and its overlap with ThrbCRM1-GFP in the electroporated population (Figures S1G–S1J). When we analyzed endogenously expressing *cThrb* RNA cells, we found that 90.7% ± 3.3% of these cells were also positive for GFP driven by the ThrbCRM1 element (Figure S1K). In contrast, the population of electroporated cells that did not express *cThrb* mRNA endogenously was very rarely positive for ThrbCRM1-GFP (1.4% ± 0.1% of cells, Figure S1K). Thus, the ThrbCRM1 element recapitulates, with high fidelity, the early expression of *cThrb* in the developing retina.

While the activity of the ThrbCRM1 in early Visinin-positive cells allowed us to identify these cells as photoreceptors, the expression of Visinin in both cones and rods and the lack of precise birthdating data regarding these cell types in chick did not allow us to definitively identify these cells as cones (Fischer et al., 2004). In the mouse retina, more precise birthdating has established that cones are born almost entirely during the embryonic period while rods are born both embryonically and postnatally, with their peak genesis near or at P0 (Carter-Dawson and LaVail, 1979). Because our electroporation protocol does not result in expression in many cells that were postmitotic at the time of DNA introduction, electroporation of P0 mouse retinas should target only rods and other cell types born postnatally (Matsuda and Cepko, 2004). Electroporation at E13.5, a time of active cone genesis, resulted in robust activity of ThrbCRM1, the ThrbICR, and a positive control, the RBP3 promoter element, which is active in both cones and rods (Figure S2A–S2D). In contrast, electroporation at P0 of these same plasmids showed no Thrb reporter expression but did show robust expression of the RBP3 reporter (Figures S2E–S2H). An additional prediction for ThrbCRM1 and ThrbICR, if they accurately represent the expression of the *Thrb* gene, is that they should not be derepressed in the *Nrl* KO retina, as *Thrb* was not derepressed (Figure 1B). This was indeed the case (Figures S2I–S2L).

ThrbCRM1 Is Active in an RPC that Generates HCs and Photoreceptors

ThrbCRM1 is active in cells other than newborn photoreceptors. The position and morphology of some of these cells was reminiscent of developing HCs (Figures 2E and 2E′, yellow arrow) (Edqvist and Hallböök, 2004). Indeed, a large number of reporter-positive cells colocalized with Lim1, a specific marker of HCs, suggesting that ThrbCRM1 was active in newborn HCs and/or the RPC that gave rise to HCs (Figures S2M–S2Q) (Liu et al., 2000).

cThrb expression has been localized to a subset of RPCs (Trimarchi et al., 2008). The position and morphology of a subset of ThrbCRM1-reporter-positive cells suggested they could be these RPCs (Figure 2E′, white arrow). To test this, ThrbCRM1-EGFP was introduced into E5 retinas, and the next day the thymidine analog 5-ethynyl-2′-deoxyuridine (EdU) was introduced for 1 hr before tissue harvest. This short EdU exposure would be expected to label RPCs in S phase and in early G2 but not postmitotic cells. Like *cThrb* mRNA, a subset of EdU-positive RPCs were ThrbCRM1-GFP positive (Figures S2R–S2V).

One model for the expression of ThrbCRM1-GFP in a subset of RPCs, HCs, and photoreceptor cells is that ThrbCRM1-GFP is active in RPCs that are heavily biased to generate cones and HCs. Intriguingly, we recently discovered such an RPC in the mouse. A knockin allele of *Olig2* that places the avian viral receptor TVA under the regulatory sequences of the *Olig2* locus was used (Hafler et al., 2012). Infection with EnvA-coated retroviruses, which require TVA for viral entry, infected only those cells that have TVA (*Olig2*-positive cells). Because the type of retrovirus used in this experiment was a gammaretrovirus, which requires the nuclear envelope breakdown that occurs during mitosis in order to integrate into the genome, only cells derived from an *Olig2*-positive RPC were labeled (i.e., postmitotic cells that expressed TVA would not lead to viral integration and expression) (Roe et al., 1993). When infection was carried out in vivo at E13.5, *Olig2*-derived clones were almost exclusively composed of cones, HCs, or both cell types, identifying this RPC type as an RPC[CH].

To test whether ThrbCRM1-positve RPCs are functionally equivalent to the *Olig2*-positive RPCs of the embryonic mouse retina, we employed a TVA/EnvA-like strategy in the chicken retina using CAT1/gp70 instead. CAT1 confers susceptibility to viruses carrying the ecotropic Moloney murine leukemia virus gp70 envelope protein and is not expressed in chickens, but when expressed in chickens it allows for gp70-mediated retrovirus infection (Albritton et al., 1989; Gotoh et al., 2011). Constructs were made with different enhancer/promoter regions placed upstream of the CAT1 coding sequence. The negative control comprised a basal promoter with no enhancer sequences, while the positive control used the CAG enhancer/promoter construct, which should provide ubiquitous expression. The ThrbCRM1 enhancer in conjunction with the same basal promoter comprised the third construct. Constructs were electroporated into E5 chicken retinas with a coelectroporation control and were infected 6 hr later with MMLV gp70- coated retroviruses encoding a GFP reporter. Retinas were assayed for GFP expression 36 hr after infection.

In retinas electroporated with the basal promoter CAT1, very few GFP-positive cells (two cells out of three retinas) were observed (Figures 2H and 2H′). In contrast, retinas electroporated with CAG-CAT1 had large patches of GFP-positive-infected cells (Figures 2I and 2I′). Interestingly, introduction of the ThrbCRM1-CAT1 receptor construct revealed isolated one- or two-cell virally labeled clones (Figures 2J and 2J′). The ThrbCRM1-derived cells were found primarily in the developing photoreceptor layer or in the vicinity of developing HCs. To determine if ThrbCRM1-derived cells preferentially assumed the photoreceptor or HC fate, specific markers of these cells (Visinin for photoreceptors and Lim1 for HCs) were applied

(Figures 2K–2R). A significant enrichment for both photoreceptors (~10-fold) and HCs (~3-fold) was observed from CAT1 expression driven by the ThrbCRM1 element compared to the CAG element (Figure 2S). This experiment demonstrates that the ThrbCRM1-positive RPC is biased to the production of these two cell types and corresponds to an RPC[CH].

Otx2, Olig2, and Onecut Family Members Are Coexpressed in RPCs

To determine which transcription factors might regulate the activity of ThrbCRM1, we examined the sequence of the 40 bp critical region of ThrbCRM1. Analysis of the sequence by Transfac suggested that the 8 bp sequence shared with ThrbICR could be regulated by the Onecut family of transcription factors (Figures S1B and S1C). Intriguingly, Onecut1 (OC1) and Onecut2 (OC2) expression has recently been localized to embryonic RPCs during the period of cone and HC genesis but not in late embryonic and postnatal RPCs (Wu et al., 2012). This restricted expression pattern makes these factors excellent candidates for regulating *Thrb*, and possibly other genes, in an RPC[CH]. Furthermore, the DNA binding domains of OC1 and OC2 are very similar (Cut and Homeodomain DNA-binding domains are 98.7% and 90.9% identical between mouse OC1 and OC2, suggesting they may transcriptionally regulate a redundant set of targets; see Bioinformatics in Experimental Procedures). At later time points and into the postnatal period, the Onecut (OC) genes are expressed in HCs at a level much higher than that seen in RPCs (Wu et al., 2012). Additionally, the sequence on either side of the predicted OC binding site closely matched a predicted Otx2 binding site (Figure S1B). As *Otx2* is a gene necessary for both HC and photoreceptor development and is expressed in embryonic RPCs, it too was an excellent candidate for regulating the ThrbCRM1 element (Emerson and Cepko, 2011; Muranishi et al., 2011; Nishida et al., 2003; Sato et al., 2007).

If Otx2 and OC factors collaborate to regulate the ThrbCRM1 element in RPC[CH]s, it would be expected that they would be expressed in the same RPCs. Examination of RPCs (as identified by EdU labeling) in the embryonic mouse revealed that a large number of Otx2-expressing RPCs also expressed OC1 and OC2 (Figures 3A–3P). To determine if OC factors were present in the RPC[CH], Olig2-positive RPCs were examined and OC2 was found to be expressed in these cells (OC1 and Olig2 colocalization could not be tested because the antibodies were from the same host) (Figures 3Q–3U). In addition, examination of the chicken retina revealed Olig2/Otx2 double-positive cells (Figures S3A–S3J) and Otx2/OC1 double-positive cells (Figures S3K–S3Y). Some of the Otx2/OC1 double-positive cells were also positive for Visinin, suggesting that OC1 is maintained in postmitotic cones for some time, in agreement with a previous study in the mouse (Figure S3U–S3Y) (Muranishi et al., 2010).

Onecut1 Is Sufficient to Induce the ThrbCRM1 Reporter Activity in the Postnatal Retina in an Otx2-Dependent Manner

OC1 and OC2 are both expressed in mouse RPCs at E12.5 and E14.5 but cease to be in RPCs after E16.5 (Wu et al., 2012). We hypothesized that the expression of OC1 and OC2 may be the molecular correlates of the competence window that restricts the production of cones and HCs to the embryonic retina. While OC1 and OC2 are no longer present in RPCs of the postnatal retina, Otx2 is still expressed in a large number of postnatally produced cells. To investigate whether an OC/Otx2 complex could regulate the ThrbCRM1 element, mouse OC1 was introduced into RPCs of the postnatal mouse retina with a ThrbCRM1-PLAP reporter. Robust PLAP expression was induced by OC1 expression but not by mOtx2, mNeuroD1, or mNeuroD6 (Figures S4A–S4H and S4A′–S4H′). The lack of activation by mOtx2, given its ability to induce ThrbCRM1 reporter in other contexts (see Figure 4), suggests that mOtx2 requires a partner in order to initiate transcription, presumably an OC family member.

To confirm the PLAP reporter results and to further examine this induction, the ThrbCRM1 reporter was coelectroporated with or without mOC1 and GFP reporter expression was analyzed in retinal sections. Confirming observations made with the PLAP reporter, GFP reporter induction was absent in wild-type (WT) retinas (Figures S4I and S4I′). The addition of CAG-mOC1 led to a large increase in GFP-positive cells found throughout the electroporated retinal patch (Figures S4J and S4J′). To investigate the possibility that the ability of mOC1 to induce the ThrbCRM1 reporter was dependent upon interaction with mOtx2, CAG-mOC1 was introduced into the P0 retina of *Otx2*Flox/Flox mice (Tian et al., 2002). When CAG-Cre was also introduced to remove *Otx2* in electroporated cells, the number of ThrbCRM1 reporter-positive cells was significantly decreased by 87.8% compared to retinas that did not receive CAG-Cre (Figure S4K). This supports the hypothesis that Otx2 is required for the activation of the ThrbCRM1 element by mOC1.

Otx2 Induction of ThrbCRM1 Reporter and Thrb mRNA in the Spinal Cord

The fact that mOC1 was sufficient to induce the ThrbCRM1 reporter in the high Otx2 expression environment of the P0 mouse retina prompted the converse question: is mOtx2 sufficient for the induction of the reporter in an OC-positive environment? To address this, we used the spinal cord, which has been shown to express all three OC family members, but has not been reported to express Otx2 (Francius and Clotman, 2010). When chicken E3 spinal cords were electroporated with the ThrbCRM1 reporter, no reporter induction was detected, suggesting that critical regulatory factors were absent (Figures 4A–4D). It was also confirmed that spinal cord expression of Otx2 could not be detected by immunohistochemistry, while OC1 was confirmed to be present (Figures 4B and 4C). Electroporation of CAG-mOC1 with the ThrbCRM1 reporter was ineffective at inducing reporter expression (Figures 4E–4H). Given the robust expression from ThrbCRM1 reporters in the mouse P0 retina coelectroporated with the mOC1 construct (Figures S4A and S4B), this clearly shows the context-dependent nature of OC activity, which is likely linked to Otx2 expression. To test this hypothesis, mOtx2 was coelectroporated with the reporter into the spinal cord. Induction of the ThrbCRM1 reporter was observed (Figures 4I–4L). As was mentioned, OC2 and OC3, which were not visualized in this experiment, also are candidates for cooperation with Otx2. When mOtx2 and mOC1 were both introduced, a clear and robust upregulation of the reporter was observed (Figures 4M–4P).

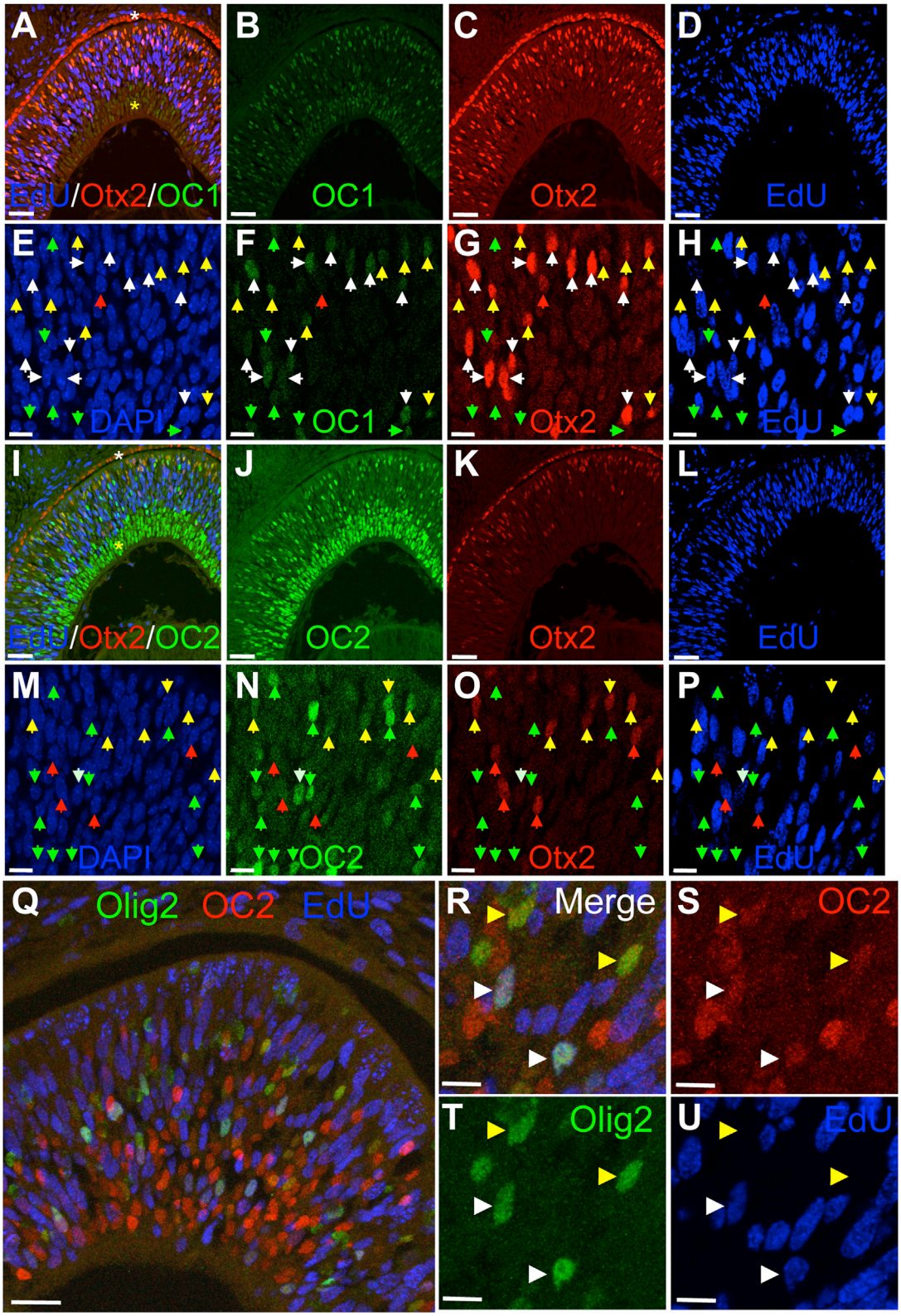

Figure 3. Otx2 Is Coexpressed with Onecut1 and Onecut2 in Mouse RPCs, and Onecut2 Is Expressed in Embryonic Olig2+ RPCs

E13.5 mouse retinas were exposed in utero to EdU for 2.5 hr before harvest and immunohistochemical analysis.

(A–D) Sections were imaged for OC1 (green), Otx2 (red), EdU (blue), and DAPI (not shown). Shown is (A) a merge of the three channels, (B) OC1, (C) Otx2, and (D) EdU.

(legend continued on next page)

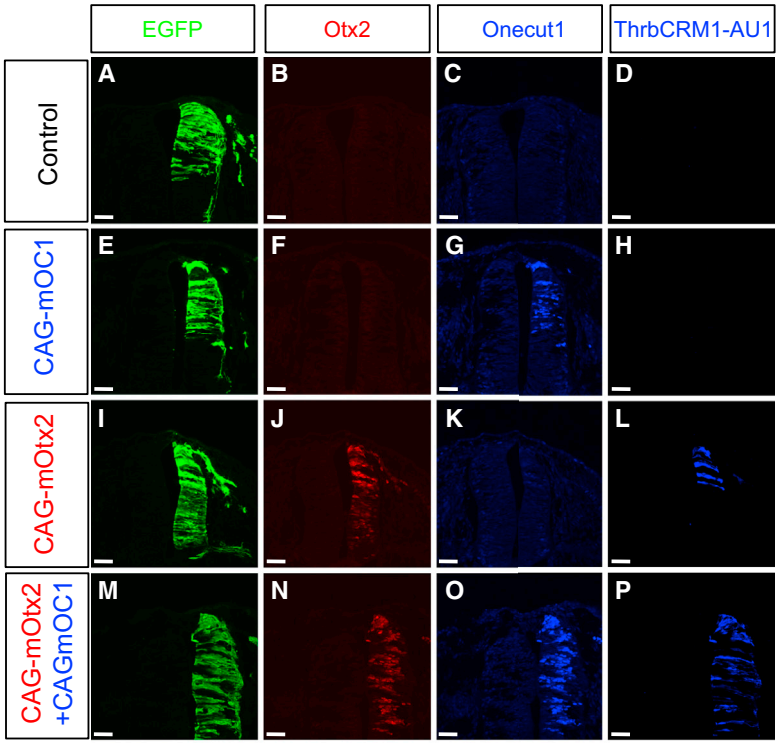

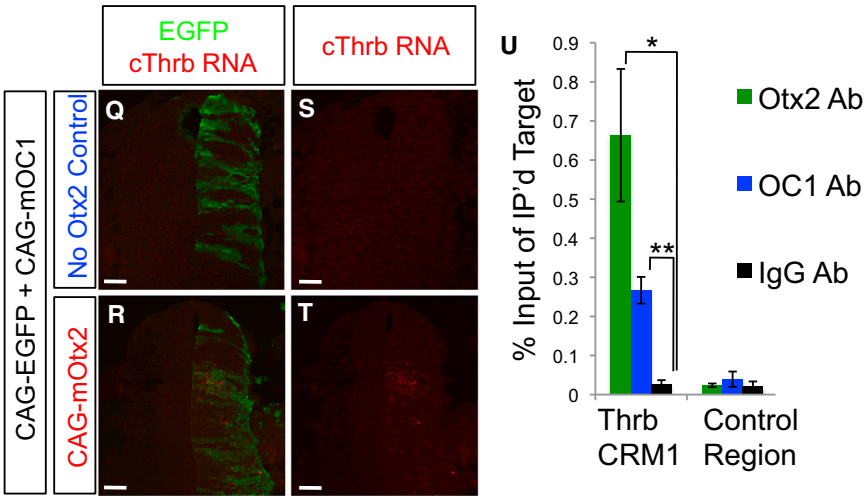

Figure 4. Effects of Spinal Cord Misexpression of mOC1 and mOtx2 on the ThrbCRM1 Reporter and cThrb Endogenous Gene Expression

(A–P) Chicken spinal cords were electroporated with CAG-EGFP and ThrbCRM1-AU1, and the misexpression plasmid is listed to the left of each row. Spinal cord sections were processed for detection of EGFP (green), Otx2 (red), OC1 (blue), and AU1 (blue).

(Q and R) Spinal cords were electroporated with the plasmids shown to the left of the rows and processed for detection of *cThrb* RNA (red) and EGFP (green).

(S and T) Shown is the *cThrb* RNA signal alone. Dorsal is the top of the section. Similar results were found for $n \geq 3$ spinal cords for each experiment.

(U) A graph of the amount of the target DNA region noted on the x axis immunoprecipitated by antibodies to Otx2 (green bars), OC1 (blue bars), and normal rabbit IgG (black bars). The y axis represents the amount immunoprecipitated as a percentage of the total chromatin input. Bars represent the averages of three biological replicates for each condition. Error bars represent SEM. A two-tailed t test showed statistically significant differences between some samples (*$p < 0.02$; **$p < 0.005$). Scale bar represents 40 μm.

See also Figure S4.

To test whether endogenous *Thrb* might be regulated by these factors, CAG-EGFP and CAG-mOC1 were coelectroporated with or without a CAG-mOtx2 construct. Detection of endogenous *cThrb* mRNA by fluorescent in situ hybridization revealed a clear upregulation of *cThrb* mRNA when mOtx2 was present (Figures 4Q–4T). This upregulation was not seen in conditions where only mOC1 was electroporated. These data suggest that mOC1, in the absence of mOtx2, is not sufficient to induce *cThrb*.

Onecut1 and Otx2 Occupy the ThrbCRM1 Element In Vivo

To determine whether Otx2 and OC1 bind in vivo to the ThrbCRM1 sequence, we used a chromatin immunoprecipitation (ChIP) assay. When antibodies to Otx2 and OC1 were used to immunoprecipitate their targets after crosslinking to DNA, a significant enrichment in the ThrbCRM1 element was found for both Otx2 and OC1 over that found when a control immunoglobulin G (IgG) antibody was used (Figure 4U). Furthermore, a control region lacking predicted Otx2 and OC1 binding sites was not significantly enriched in either Otx2 or OC1 immunoprecipitations (Figure 4U). These data show that Otx2 and OC1

(E–H) Single z-plane images of each channel as denoted. Green arrows (OC1+ only), red arrows (Otx2+ only), yellow arrows (Otx2+/OC1+), and white arrows (Otx2+/OC1+/EdU+) point to specific cells. The white asterisk marks Otx2+ RPE, and the yellow asterisk marks the OC1+ retinal ganglion cell layer.

(I–P) Same as in (A)–(H) but imaged for OC2 (green) instead of OC1.

(Q) Imaged for Olig2 (green), OC2 (red), and EdU (blue).

(R–U) High-magnification view of retina processed as in (Q), with channels denoted.

The white arrows (Olig2+/OC2+/EdU+) and yellow arrows (Olig2+/OC2+) point to specific cells. Scale bar represents 40 μm for (A)–(D), (I)–(L), and (Q) and 10 μm for (E)–(H), (M)–(P), and (R)–(U).

See also Figure S3.

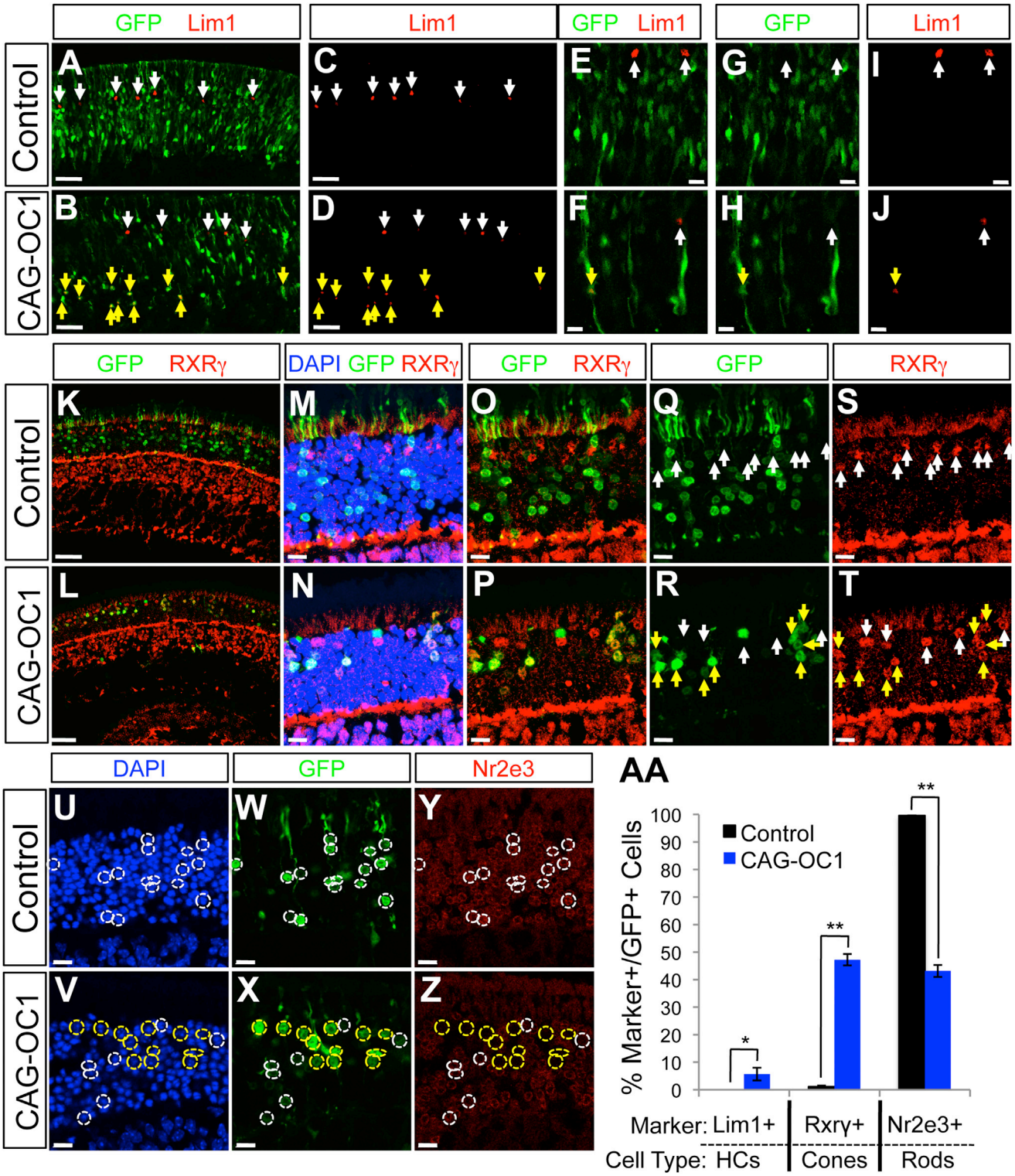

Figure 5. mOC1 Misexpression in the Postnatal Mouse Retina Induces HC and Cone Gene Expression and Inhibits Rod Differentiation

Mouse P0 retinas were electroporated in vivo with CAG-EGFP, with or without CAG-mOC1. The channels shown in each panel are denoted at the top of each column and the presence or absence of mOC1 to the left of each row.

(A–J) Shown are retinas harvested at P4. The white arrows point to Lim1+ cells that were not electroporated (EGFP−), corresponding to the normally generated HCs, and the yellow arrows point to EGFP+/Lim1+ cells. (E–J) High-magnification single z-section images.

(K–T) Shown are retinas harvested at P30. The white arrows point to RXRγ+ cells that were not electroporated (EGFP−), corresponding to normally generated cones, and the yellow arrows point to EGFP+/RXRγ+ cells.

(legend continued on next page)

specifically occupy the ThrbCRM1 element in vivo and support their dual regulation of *cThrb* expression.

Onecut1 Is Sufficient to Extend the Competence Window for Genesis of Cone Photoreceptors and HCs to the Postnatal Period

mOC1/mOtx2 could control just the expression of *Thrb*, or these genes could act more broadly to establish the RPC[CH] state. To investigate this possibility, mOC1 was introduced into postnatal mouse RPCs and the expression of cone and HC markers was assessed. A significant increase in cells positive for Lim1, a specific marker of HCs, was observed in the electroporated population only when mOC1 was introduced (Figures 5A–5J and 5AA). These cells localized near the vitreal side of the inner nuclear layer (INL), where HCs migrate to when they are born. Introduction of CAG-mOC1 also resulted in the significant production of RXRγ-positive cells in the developing photoreceptor layer (Figures 5K–5T and 5AA). While RXRγ also marks RGCs, the position and morphology of these cells and their continued expression of Otx2 (data not shown) strongly suggested that these are induced cones. These GFP-positive/ RXRγ-positive cells were also present at P4 and P21 (data not shown). Furthermore, examination of Nr2e3, an exclusive marker of rods in the adult retina (Chen et al., 2005), revealed that mOC1 expression significantly reduced the number of Nr2e3-positive cells in the ONL (Figures 5U–5Z and 5AA). Thus, these data support the hypothesis that the expression of mOC1/mOtx2 can shift the competence window of cone and HC production to the postnatal period and also suppress the expression of rod photoreceptor markers.

Interference with Onecut Transcription Activity Leads to an Increase in Rods

The necessity of OC factors in retinal development was investigated using methods to reduce their expression and/or activity. Several outcomes were considered. One outcome concerns photoreceptors: would they be made, and would they be cones? If OC family members function like Otx2, then reduction of OC activity would lead to fates other than photoreceptors, such as amacrine cells. Alternatively, if absence of OC family members allowed for Otx2 to still drive the production of photoreceptors, then rods, but not cones, might be formed. This is the situation in the postnatal mouse retina, when Otx2 is present but OCs are absent from RPCs.

To investigate the function of OC1 in the chicken retina, a dominant-negative approach was taken. The engrailed repressor (EnR) domain was fused to the DNA binding domain of mOC1, either N terminally (EnR-OC1) or C terminally (OC1-EnR), and these constructs were introduced into E5 chick retinas. Expression from the ThrbCRM1-PLAP reporter was used to assess their predicted effect. Both OC1-EnR and EnR-OC1 fusions led to a large decrease in reporter activity compared to the expression of ThrbCRM1 alone (Figures 6A–6C and 6A′–6C′). No observable effects on ThrbCRM1 reporter activity were observed when either the EnR domain or the OC1-DBD domain by themselves were tested (Figures 6D, 6E, 6D′, and 6E′).

The effects of these dominant-negative constructs on cell fates were then assessed. The expression of a coelectroporated RBP3 element, which is active in both early cones and rods, was tested. In contrast to what was observed with the ThrbCRM1 reporter, the expression of the RBP3 reporter was unaffected by OC1-EnR, suggesting that photoreceptors were still generated (data not shown). Interestingly, the Rhodopsin promoter was activated in a premature manner by coelectroporation with OC1-EnR (Figure S5). This strongly suggests that interference with OC target proteins leads to the premature specification of rods.

To test whether endogenous gene expression might support such a model, the expression of *L-Maf* (also known as *MafA*) was determined. *L-Maf* is the earliest known marker of rods in the chicken that allows for the distinction between cones and rods (Ochi et al., 2004). In the mouse and human retina, *Nrl* is another Maf family transcription factor that is also the earliest known marker of rods (Akimoto et al., 2006). Importantly, these factors are thought to be critical for the expression of Rhodopsin, and thus L-Maf upregulation might explain the effects observed on the Rhodopsin promoter (Mears et al., 2001; Rehemtulla et al., 1996). To test this, retinas were electroporated with the EnR constructs and *L-Maf* expression was examined. Upregulation of *L-Maf* RNA was observed in response to both OC1-EnR and EnR-OC1 compared to either the addition of no EnR construct or the EnR by itself (Figures 6F–6I and 6F′–6I′). Interestingly, electroporation of just the OC1DBD domain induced the production of some *L-Maf*-positive cells (Figures 6J and 6J′). This is not unexpected, as the OC1DBD domain could act as a dominant negative that blocks the binding of endogenous OC family members. It was also notable that *L-Maf*-positive cells were in a position and with a morphology suggestive of early rods. This suggests that OC1-EnR does not upregulate *L-Maf* in any electroporated cell type or convert all RPCs to rods but may be converting to rods only the cells already delimited by Otx2 and/or other factors to become photoreceptors. Taken together, these results suggest that the OC1-EnR constructs specifically lead to upregulation of *L-Maf* and likely the rod fate.

Alterations in Early Cone and Rod Photoreceptor Markers in the Onecut1 Knockout Mouse

To assess whether the apparent photoreceptor fate changes observed in the chicken retina in response to interfering with OC function could be confirmed in the mouse retina, the *OC1* KO mouse was examined (Jacquemin et al., 2000). Despite the large overlap in the expression of OC1 and OC2 observed in embryonic RPCs, we tested whether these genes might not be

(U–Z) Shown are retinas harvested at P30. White dotted lines encompass EGFP+/Nr2e3+ nuclei and yellow dotted lines GFP+/Nr2e3− nuclei.
(AA) Quantitation of the overlap of CAG-GFP with the marker listed along the x axis in either control (black bars) or CAG-OC1 (blue bars) electroporated retinas (as in A–Z). The cell type normally associated with that marker expression and location is given below the markers. Values represent the percentage of marker-positive cells among the GFP-positive cells (for Nr2e3 and RXRγ, only the ONL population was counted) and are the average from three retinas. Error bars represent SEM. Statistical significance was determined by t test (*$p < 0.05$ using a one-tailed t test; **$p < 0.0001$ using a two-tailed t test).
Scale bar represents 10 μm in (E)–(J), (M)–(T), and (W)–(D′) and 40 μm in (A)–(D), (K), (L), (U), and (V).

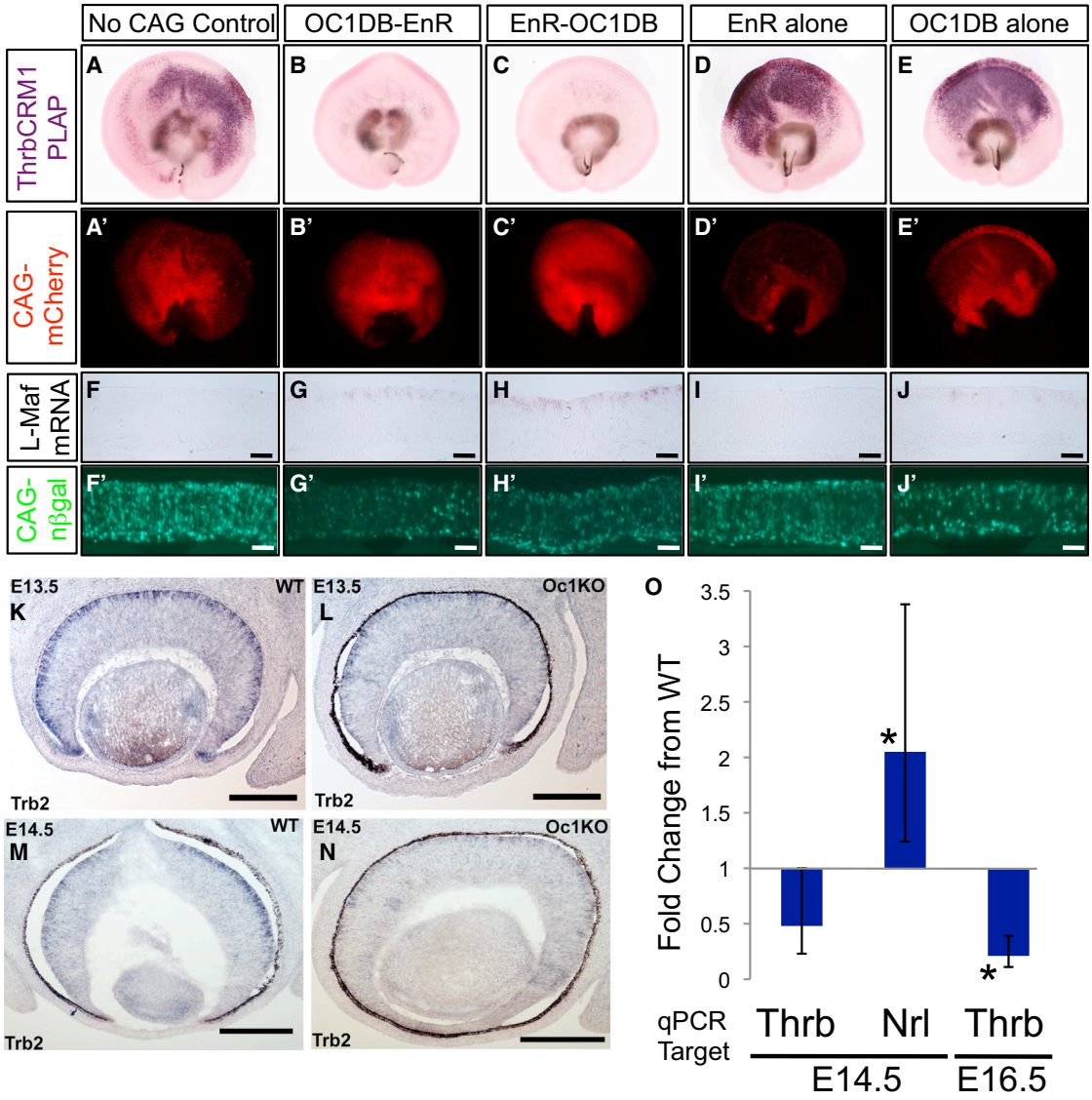

Figure 6. Interference with Onecut Transcriptional Activity in Both Chickens and Mice Leads to Downregulation of ThrbCRM1/Thrb mRNA Expression and Upregulation of Rod Photoreceptor Gene *Nrl*/*L-Maf*

(A–E) E5 chicken retinas were electroporated with CAG-mCherry, ThrbCRM1-PLAP, and the CAG construct noted at the top of each column and developed for PLAP activity 2 days later.

(A′–E′) CAG-mCherry visualization of the retinas shown above.

(F–J) E5 retinas were electroporated with CAG-nβ-gal (and the CAG construct is shown at the top of each column), cultured for 3 days, and processed for RNA in situ hybridization to detect *L-Maf* as shown by alkaline phosphatase staining. Biological replicates and experiments with a different probe to *L-Maf* gave the same result.

(F′–J′) β-gal expression for the sections in (F)–(J).

(K–N) RNA in situ hybridization to detect mThrb expression in the embryonic retina of WT (K and M) and OC1 KO mice (L and N) at E13.5 and E14.5.

(O) qPCR analysis of *Thrb* and *Nrl* expression in the embryonic retinas graphed as the fold change of the RNA listed along the x axis in *OC1* KO mice relative to WT mice at E14.5 and E16.5. Error bars represent SEM. N ≥ 3 animals per genotype. Asterisks denote $p < 0.01$ using a two-tailed t test.

Scale bar represents 25 μm for (F)–(J) and (F′)–(J′) and 100 μm for (K–N). See also Figure S5.

completely functionally redundant (Wu et al., 2012). At both E13.5 and E14.5, there was an observable reduction of *Thrb* mRNA in the OC1 KO retina, providing support that *Thrb* is an in vivo transcriptional target of mOC1 (Figures 6K–6N). At both E14.5 and E16.5, a clear reduction in *Thrb* levels, as analyzed by qPCR, was observed that was statistically significant at E16.5 ($p < 0.01$) (Figure 6O). As the OC1-EnR data in the chicken suggested that rod genesis might be upregulated in the *OC1* KO mice, the distribution of the early rod marker *Nrl* was assessed. Indeed, *OC1* KOs had a greater than 2-fold increase in the expression of *Nrl* relative to WT mice ($p < 0.01$) (Figure 6O). These data were supported by the fact that

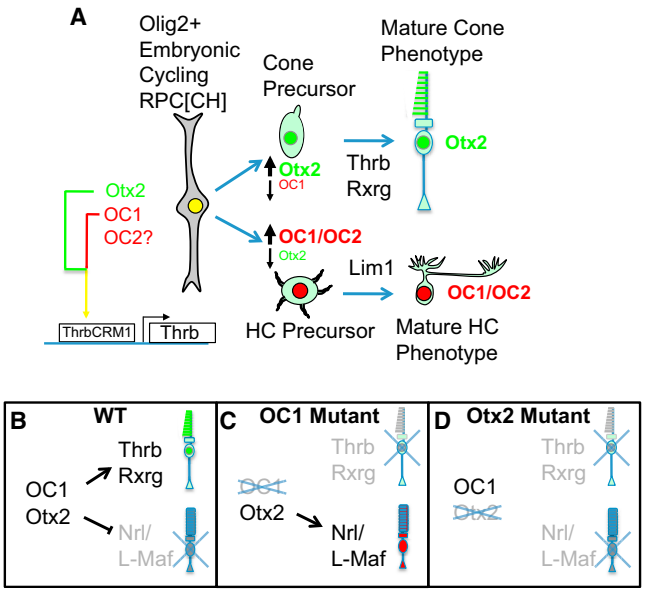

Figure 7. Models for the Roles of Otx2 and Onecut Factors in Horizontal Cell and Photoreceptor Genesis

(A) A model for OC1 and Otx2 action in the retina is shown. The RPC[CH] divides to give rise to cones and HCs. In cone precursor cells, the level of OC1 declines and Otx2 is maintained while in HC precursors, the level of OC1 increases and Otx2 decreases. OC2 may be functionally redundant with OC1 in RPC[CH]s.

(B) In WT RPCs, coexpression of Otx2 and OC1 promotes cone genesis (green cells) and inhibits rod genesis (red cells).

(C) In *OC1* mutants, rod genesis is promoted and cone genesis is impaired.

(D) In *Otx2* mutants, all photoreceptor genesis is inhibited and amacrine cells are generated instead.

two independent microarrays of *OC1* KO mice also had a greater than 2-fold induction of *Nrl* compared to WT mice at E14.5 (J.J.G. and J.T., unpublished data). Thus, OC1 in the mouse retina normally suppresses early rod photoreceptor gene expression.

DISCUSSION

The data presented here demonstrate that the ThrbCRM1 element defines a specific RPC that that is heavily biased to the production of cones and HCs (Figure 7A). We previously reported that the E13.5 mouse RPCs that express *Olig2* produce only cones and HCs (Hafler et al., 2012). However, unlike *Olig2*, which did not lead to a phenotype when removed in the mouse (Hafler et al., 2012), *OC1* is a critical factor that defines the competence for cone and HC production. Moreover, OC1 was shown to act genetically upstream of *Nrl* to control the rod versus cone fate choice (Figures 7B and 7C). Given the transient expression in newborn cones, OC1 is not likely to activate later cone-specific gene expression but instead to initiate a cascade that promotes cone differentiation. This is in accord with analysis of the *Nrl* KO mouse, in which there is no evidence from microarray studies that Onecut genes are upregulated (Yoshida et al., 2004). Thus, the cone-specific genes dysregulated in *Nrl* KO mice must be controlled by other regulatory factors. One of these factors is the Spalt family transcription factor, Sall3, which was recently identified as a regulator of HC and cone differentiation and is upregulated in the *Nrl* KO mouse (de Melo et al., 2011; Yoshida et al., 2004). The fact that Sall3 does not lead to expression of Lim1 or Rxrg, as OC1 does, and is expressed late in HCs and cones suggests that Sall3 is genetically downstream of OC1. Interestingly, we found that misexpressed OC1 can induce the early markers of cones but fails to induce the late ones. This may be due to the fact that the CAG promoter used to misexpress OC1 leads to sustained OC1 expression, while OC1 expression normally goes down as cones mature. This sustained expression may interfere with the progression of photoreceptors beyond the Thrb/Rxrg stage (data not shown). Thus, the regulatory events that allow for complete cone differentiation initiated by OC1 and Otx2 need to be clarified but may involve bHLH genes, along with other transcription factors, which may each regulate a subset of photoreceptor-specific genes. Our data also suggest that OC1 does not directly repress *L-Maf*, as the EnR-Oc1DBD led to derepression of *L-Maf*. This would predict an as-yet-unidentified protein positively regulated by OC1 that represses *L-Maf* in chickens and presumably one in mammals that regulates *Nrl*.

Although OC1 has been most closely associated with liver gene regulation, several recent studies have identified OC factors as specific cell-fate regulators in the spinal cord (motoneurons) and mesencephalic trigeminal nucleus (Espana and Clotman, 2012; Francius and Clotman, 2010; Samadani and Costa, 1996). In the retina, the data presented here suggest that the specificity of OC1 transcriptional targets in the retina is due to cooperation with Otx2. That is, cones and HCs are not generated in the spinal cord, where OC1 is found, due to the lack of Otx2. Introduction of Otx2 into the spinal cord is capable of activating the ThrbCRM1 reporter and endogenous *Thrb* expression. Thus, coexpression of Otx2 and OC1 may be sufficient to drive early events in cone genesis, suggesting their applicability in cone induction from stem cells. It will also be critical to examine whether OC factors, in collaboration with other factors or acting alone, influence the development of other cell types in the retina in addition to photoreceptors and HCs. Given the overlap in expression and sequence homology of OC1 and OC2, future studies also will be needed to determine if these genes have a redundant function in the retina (Wu et al., 2012).

The network elements described here may also be conserved in *Drosophila*. The *Drosophila* homolog of Otx, *otd*, is important in *Drosophila* photoreceptor development (Vandendries et al., 1996). The *Drosophila* OC gene has DNA-binding domains that are highly related to the vertebrate homologs, is expressed in *Drosophila* photoreceptors, and can bind to the *Drosophila* rhodopsin enhancer (Nguyen et al., 2000). Thus, it will be interesting to explore whether *otd* and OC have an evolutionarily conserved role in driving photoreceptor development.

The vertebrate retina comprises approximately 60 different cell types (reviewed in Masland, 2011). This diverse group of cells is generated by a pool of RPCs, many of which were shown to be multipotent throughout development (Holt et al., 1988; Turner and Cepko, 1987; Turner et al., 1990; Wetts and Fraser, 1988). While clonal lineage analyses showed the multipotential nature of RPCs, the same analyses showed a great diversity in clone types, originating even from a single time in development.

This observation raised the possibility that even though RPCs are multipotent, they may not be equivalent and may differ in their potential for proliferation and in their ability to make different cell types. Evidence for distinct types of RPCs has accumulated over the last few years (Brzezinski et al., 2011; Godinho et al., 2007; Hafler et al., 2012; Rompani and Cepko, 2008), including one recent study in which we found that embryonic mouse RPCs that express the bHLH transcription factor *Olig2* divide only once and produce cones and HCs (Hafler et al., 2012). Our current study has now identified key factors that endow *Olig2*+ RPCs with the ability to make these types of daughter cells. Otx2 and OC factors are coexpressed in Olig2+ RPCs during early embryonic retinal development, when cones and HCs are made, but are not coexpressed in late embryonic or postnatal Olig2+ RPCs, when rods and amacrine cells are made by Olig2+ RPCs (Figure 7A). After cones and HCs are generated, the coexpression of Otx2 and OC factors resolves such that cones express Otx2, but not OCs, and HCs express OCs, but not Otx2 (Figure 7A). This lack of Otx2 expression in HCs led to an ambiguity in our understanding of the phenotype of the *Otx2* KO mouse. In the *Otx2* conditional KO mouse, cones and rods, as well as HCs and bipolar cells, are not generated (Figure 7D) (Nishida et al., 2003; Sato et al., 2007). The reason for this defect in HC development can now be ascribed to a role of Otx2 in the RPC[CH] and/or newly postmitotic cells generated by these RPCs. There must be a regulatory relationship that resolves the upregulation and downregulation of OCs and Otx2 as differentiation proceeds in cones and HCs. Examination of the CRMs of these and other genes involved in the development of these cell types at these time points should provide candidates for this network.

EXPERIMENTAL PROCEDURES

Bioinformatics

Candidate CRMs were identified and analyzed as previously described (Emerson and Cepko, 2011). Binding site logos were from Transfac (Matys et al., 2006). NP_032288.1(mOC1) and NP_919244.2 (mOC2) protein sequences from the National Center for Biotechnology Information were compared using the ClustalW program.

DNA Electroporations

Ex vivo and in vivo retina electroporations were carried out as described previously (Cherry et al., 2011; Emerson and Cepko, 2011). All results based on PLAP-stained retinas were repeated with a minimum of two biological replicates. Chicken in ovo spinal cord electroporations used stage 18 embryos at the thoracic level (0.5 μg/μl for CAG constructs and 1.0 μg/μl for ThrbCRM1-AU1). The spinal cord was flanked by a sharp tungsten electrode inserted into the embryo and a gold-plated positive electrode on the right side. Three pulses of 10 V, 50 ms each and 950 ms apart, were applied and embryos were harvested the next day and processed according to our retinal procedure. P0–P30 electroporations used a floxed version of CAG-OC1 described in the Supplemental Experimental Procedures.

Immunohistochemistry

Antibody sources, concentrations, and conditions were used as previously described (Emerson and Cepko, 2011) and can be found in the Supplemental Experimental Procedures. EdU labeling was performed by injecting pregnant dams with 150 μl of 10 mg/ml EdU resuspended in 1× PBS. EdU detection was performed with a Click-iT EdU Alexa Fluor 647 imaging kit (C10340, Invitrogen).

Section RNA In Situ Hybridization

See Supplemental Experimental Procedures for RNA probe generation. *mThrb* and *cThrb* RNA detection by alkaline phosphatase development methodology was as described elsewhere (Trimarchi et al., 2007). Fluorescent *cThrb* RNA detection used anti-digoxigenin (DIG) coupled to POD and several washes in TNT were performed after antibody incubation and MABT washes. Slides processed for tyramide amplification used Cy3-tyramide (1:100, Perkin Elmer) for 20 min, washed three times in TNT and once in 1× PBS plus 0.1% Tween-20, and processed for GFP. Methodology for *L-Maf* RNA hybridization was as described previously (Trimarchi et al., 2007), except with no postfixation and the sections were further processed for β-galactosidase (β-gal) immunodetection.

Dissociated Cell In Situ Hybridization

Retinal explants were cultured ex vivo for 8 hr, digested into a single-cell suspension with papain, incubated on poly-D-lysine-coated slides (30 min, room temperature) in Dulbecco's modified Eagle's medium plus 10% fetal calf serum and fixed with 4% paraformaldehyde for 10 min. The DISH protocol was as described in Trimarchi et al. (2007), with these modifications: no methanol dehydration, α-DIG-POD was applied for 1.5 hr, and postdevelopment fixation was not performed. Slides were then processed to detect β-gal and GFP immunofluorescently and nuclei were stained with DAPI.

Chromatin Immunoprecipitation

ChIP experiments were performed with the EZ ChIP kit (Millipore, 17-371). Seven E5 retinas were used for each biological sample and triplicate biological samples were analyzed. Chromatin was prepared in a Bioruptor (Diagenode) (three pulses, each 5 min long). One-twelfth of the sample was used for each immunoprecipitation and 10 μg of each antibody (anti-Otx2, ab21990, Abcam; anti-OC1, sc-13050, Santa Cruz Biotechnology; normal rabbit IgG, sc-2027, Santa Cruz Biotechnology) was used in each immunoprecipitation. See also Supplemental Experimental Procedures.

Imaging and Image Processing

Confocal imaging was done as described previously (Emerson and Cepko, 2011); some images were taken with a Leica SP2 upright confocal. Image processing was performed with Imaris software. Images were uniformly adjusted within an image and between samples in a group. Images in Figures 2K–2R, Figures 3Q–3U, Figures S3U–S3Y, and Figures 5Q–5T use maximum-intensity projections for illustrating colocalization for presentation purposes, but colocalization was verified by single z-plane analysis for all such images. All quantitation was done as in Emerson and Cepko (2011). Retinal images are oriented with the sclerad side up.

Animals

All methods used in animal studies were approved by the Institutional Animal Care and Use Committee at Harvard University and Iowa State University.

SUPPLEMENTAL INFORMATION

Supplemental Information includes Supplemental Experimental Procedures and five figures and can be found with this article online at http://dx.doi.org/10.1016/j.devcel.2013.06.005.

ACKNOWLEDGMENTS

Fan Wang (*OC1* knockout), Anand Swaroop (*Nrl* knockout), and Shinichi Aizawa (*Otx2* floxed allele) generously provided mouse strains. We thank Gregory Martin for performing the mouse in situ hybridizations in Figure 6 and Susan Carpenter for access to her qPCR machine. Richard Mulligan kindly provided the gp70 plasmid, and Cliff Tabin provided the slax-repressor template. The 40-1a, 4F2, and Visinin antibodies developed by Joshua Sanes, Thomas Jessell and Susan Brenner-Morton, and Suzanne Bruhn were obtained from the Developmental Studies Hybridoma Bank developed under the auspices of the NICHD and maintained by the Department of Biology at The University of Iowa. Support was provided by a National Institutes of Health (NIH) National Research Service Award Kirschstein fellowship (to M.M.E.), NIH National Eye Institute grant RO1 EY009676 (to C.L.C.), and funding from the

Foundation Fighting Blindness. C.L.C. is an Investigator of the Howard Hughes Medical Institute. We thank the members of the Cepko, Tabin, and Dymecki laboratories for useful discussions and support for this project.

Received: October 27, 2012
Revised: April 22, 2013
Accepted: June 6, 2013
Published: July 15, 2013

REFERENCES

Akimoto, M., Cheng, H., Zhu, D., Brzezinski, J.A., Khanna, R., Filippova, E., Oh, E.C.T., Jing, Y., Linares, J.-L., Brooks, M., et al. (2006). Targeting of GFP to newborn rods by Nrl promoter and temporal expression profiling of flow-sorted photoreceptors. Proc. Natl. Acad. Sci. USA *103*, 3890–3895.

Albritton, L.M., Tseng, L., Scadden, D., and Cunningham, J.M. (1989). A putative murine ecotropic retrovirus receptor gene encodes a multiple membrane-spanning protein and confers susceptibility to virus infection. Cell *57*, 659–666.

Brzezinski, J.A., 4th, Kim, E.J., Johnson, J.E., and Reh, T.A. (2011). Ascl1 expression defines a subpopulation of lineage-restricted progenitors in the mammalian retina. Development *138*, 3519–3531.

Carter-Dawson, L.D., and LaVail, M.M. (1979). Rods and cones in the mouse retina. II. Autoradiographic analysis of cell generation using tritiated thymidine. J. Comp. Neurol. *188*, 263–272.

Chen, J., Rattner, A., and Nathans, J. (2005). The rod photoreceptor-specific nuclear receptor Nr2e3 represses transcription of multiple cone-specific genes. J. Neurosci. *25*, 118–129.

Cherry, T.J., Wang, S., Bormuth, I., Schwab, M., Olson, J., and Cepko, C.L. (2011). NeuroD factors regulate cell fate and neurite stratification in the developing retina. J. Neurosci. *31*, 7365–7379.

Daniele, L.L., Lillo, C., Lyubarsky, A.L., Nikonov, S.S., Philp, N., Mears, A.J., Swaroop, A., Williams, D.S., and Pugh, E.N., Jr. (2005). Cone-like morphological, molecular, and electrophysiological features of the photoreceptors of the Nrl knockout mouse. Invest. Ophthalmol. Vis. Sci. *46*, 2156–2167.

de Melo, J., Peng, G.-H., Chen, S., and Blackshaw, S. (2011). The Spalt family transcription factor Sall3 regulates the development of cone photoreceptors and retinal horizontal interneurons. Development *138*, 2325–2336.

Edqvist, P.-H.D., and Hallböök, F. (2004). Newborn horizontal cells migrate bi-directionally across the neuroepithelium during retinal development. Development *131*, 1343–1351.

Emerson, M.M., and Cepko, C.L. (2011). Identification of a retina-specific Otx2 enhancer element active in immature developing photoreceptors. Dev. Biol. *360*, 241–255.

Espana, A., and Clotman, F. (2012). Onecut factors control development of the Locus Coeruleus and of the mesencephalic trigeminal nucleus. Mol. Cell. Neurosci. *50*, 93–102.

Fischer, A.J., Wang, S.-Z., and Reh, T.A. (2004). NeuroD induces the expression of visinin and calretinin by proliferating cells derived from toxin-damaged chicken retina. Dev. Dyn. *229*, 555–563.

Fischer, A.J., Foster, S., Scott, M.A., and Sherwood, P. (2008). Transient expression of LIM-domain transcription factors is coincident with delayed maturation of photoreceptors in the chicken retina. J. Comp. Neurol. *506*, 584–603.

Francius, C., and Clotman, F. (2010). Dynamic expression of the Onecut transcription factors HNF-6, OC-2 and OC-3 during spinal motor neuron development. Neuroscience *165*, 116–129.

Gehrs, K.M., Anderson, D.H., Johnson, L.V., and Hageman, G.S. (2006). Age-related macular degeneration—emerging pathogenetic and therapeutic concepts. Ann. Med. *38*, 450–471.

Godinho, L., Williams, P.R., Claassen, Y., Provost, E., Leach, S.D., Kamermans, M., and Wong, R.O.L. (2007). Nonapical symmetric divisions underlie horizontal cell layer formation in the developing retina in vivo. Neuron *56*, 597–603.

Gotoh, H., Ono, K., Takebayashi, H., Harada, H., Nakamura, H., and Ikenaka, K. (2011). Genetically-defined lineage tracing of Nkx2.2-expressing cells in chick spinal cord. Dev. Biol. *349*, 504–511.

Hafler, B.P., Surzenko, N., Beier, K.T., Punzo, C., Trimarchi, J.M., Kong, J.H., and Cepko, C.L. (2012). Transcription factor Olig2 defines subpopulations of retinal progenitor cells biased toward specific cell fates. Proc. Natl. Acad. Sci. USA *109*, 7882–7887.

Hartong, D.T., Berson, E.L., and Dryja, T.P. (2006). Retinitis pigmentosa. Lancet *368*, 1795–1809.

Hatakeyama, J., Tomita, K., Inoue, T., and Kageyama, R. (2001). Roles of homeobox and bHLH genes in specification of a retinal cell type. Development *128*, 1313–1322.

Holt, C.E., Bertsch, T.W., Ellis, H.M., and Harris, W.A. (1988). Cellular determination in the Xenopus retina is independent of lineage and birth date. Neuron *1*, 15–26.

Hsiau, T.H.-C., Diaconu, C., Myers, C.A., Lee, J., Cepko, C.L., and Corbo, J.C. (2007). The cis-regulatory logic of the mammalian photoreceptor transcriptional network. PLoS ONE *2*, e643.

Jacquemin, P., Durviaux, S.M., Jensen, J., Godfraind, C., Gradwohl, G., Guillemot, F., Madsen, O.D., Carmeliet, P., Dewerchin, M., Collen, D., et al. (2000). Transcription factor hepatocyte nuclear factor 6 regulates pancreatic endocrine cell differentiation and controls expression of the proendocrine gene ngn3. Mol. Cell. Biol. *20*, 4445–4454.

Jadhav, A.P., Mason, H.A., and Cepko, C.L. (2006). Notch 1 inhibits photoreceptor production in the developing mammalian retina. Development *133*, 913–923.

Jones, I., Ng, L., Liu, H., and Forrest, D. (2007). An intron control region differentially regulates expression of thyroid hormone receptor beta2 in the cochlea, pituitary, and cone photoreceptors. Mol. Endocrinol. *21*, 1108–1119.

Koike, C., Nishida, A., Ueno, S., Saito, H., Sanuki, R., Sato, S., Furukawa, A., Aizawa, S., Matsuo, I., Suzuki, N., et al. (2007). Functional roles of Otx2 transcription factor in postnatal mouse retinal development. Mol. Cell. Biol. *27*, 8318–8329.

Liu, W., Wang, J.H., and Xiang, M. (2000). Specific expression of the LIM/homeodomain protein Lim-1 in horizontal cells during retinogenesis. Dev. Dyn. *217*, 320–325.

Masland, R.H. (2011). Cell populations of the retina: the Proctor lecture. Invest. Ophthalmol. Vis. Sci. *52*, 4581–4591.

Matsuda, T., and Cepko, C.L. (2004). Electroporation and RNA interference in the rodent retina in vivo and in vitro. Proc. Natl. Acad. Sci. USA *101*, 16–22.

Matys, V., Kel-Margoulis, O.V., Fricke, E., Liebich, I., Land, S., Barre-Dirrie, A., Reuter, I., Chekmenev, D., Krull, M., Hornischer, K., et al. (2006). TRANSFAC and its module TRANSCompel: transcriptional gene regulation in eukaryotes. Nucleic Acids Res. *34*(Database issue), D108–D110.

Mears, A.J., Kondo, M., Swain, P.K., Takada, Y., Bush, R.A., Saunders, T.L., Sieving, P.A., and Swaroop, A. (2001). Nrl is required for rod photoreceptor development. Nat. Genet. *29*, 447–452.

Mori, M., Ghyselinck, N.B., Chambon, P., and Mark, M. (2001). Systematic immunolocalization of retinoid receptors in developing and adult mouse eyes. Invest. Ophthalmol. Vis. Sci. *42*, 1312–1318.

Muranishi, Y., Sato, S., Inoue, T., Ueno, S., Koyasu, T., Kondo, M., and Furukawa, T. (2010). Gene expression analysis of embryonic photoreceptor precursor cells using BAC-Crx-EGFP transgenic mouse. Biochem. Biophys. Res. Commun. *392*, 317–322.

Muranishi, Y., Terada, K., Inoue, T., Katoh, K., Tsujii, T., Sanuki, R., Kurokawa, D., Aizawa, S., Tamaki, Y., and Furukawa, T. (2011). An essential role for RAX homeoprotein and NOTCH-HES signaling in Otx2 expression in embryonic retinal photoreceptor cell fate determination. J. Neurosci. *31*, 16792–16807.

Ng, L., Hurley, J.B., Dierks, B., Srinivas, M., Saltó, C., Vennström, B., Reh, T.A., and Forrest, D. (2001). A thyroid hormone receptor that is required for the development of green cone photoreceptors. Nat. Genet. *27*, 94–98.

Ng, L., Ma, M., Curran, T., and Forrest, D. (2009). Developmental expression of thyroid hormone receptor beta2 protein in cone photoreceptors in the mouse. Neuroreport *20*, 627–631.

Nguyen, D.N., Rohrbaugh, M., and Lai, Z. (2000). The Drosophila homolog of Onecut homeodomain proteins is a neural-specific transcriptional activator with a potential role in regulating neural differentiation. Mech. Dev. *97*, 57–72.

Nishida, A., Furukawa, A., Koike, C., Tano, Y., Aizawa, S., Matsuo, I., and Furukawa, T. (2003). Otx2 homeobox gene controls retinal photoreceptor cell fate and pineal gland development. Nat. Neurosci. *6*, 1255–1263.

Ochi, H., Sakagami, K., Ishii, A., Morita, N., Nishiuchi, M., Ogino, H., and Yasuda, K. (2004). Temporal expression of L-Maf and RaxL in developing chicken retina are arranged into mosaic pattern. Gene Expr. Patterns *4*, 489–494.

Oh, E.C.T., Khan, N., Novelli, E., Khanna, H., Strettoi, E., and Swaroop, A. (2007). Transformation of cone precursors to functional rod photoreceptors by bZIP transcription factor NRL. Proc. Natl. Acad. Sci. USA *104*, 1679–1684.

Ong, J.M., and da Cruz, L. (2012). A review and update on the current status of stem cell therapy and the retina. Br. Med. Bull. *102*, 133–146.

Rehemtulla, A., Warwar, R., Kumar, R., Ji, X., Zack, D.J., and Swaroop, A. (1996). The basic motif-leucine zipper transcription factor Nrl can positively regulate rhodopsin gene expression. Proc. Natl. Acad. Sci. USA *93*, 191–195.

Roberts, M.R., Hendrickson, A., McGuire, C.R., and Reh, T.A. (2005). Retinoid X receptor (gamma) is necessary to establish the S-opsin gradient in cone photoreceptors of the developing mouse retina. Invest. Ophthalmol. Vis. Sci. *46*, 2897–2904.

Rodieck, R.W. (1998). The First Steps in Seeing (Sunderland, MA: Sinauer Associates).

Roe, T., Reynolds, T.C., Yu, G., and Brown, P.O. (1993). Integration of murine leukemia virus DNA depends on mitosis. EMBO J. *12*, 2099–2108.

Rompani, S.B., and Cepko, C.L. (2008). Retinal progenitor cells can produce restricted subsets of horizontal cells. Proc. Natl. Acad. Sci. USA *105*, 192–197.

Samadani, U., and Costa, R.H. (1996). The transcriptional activator hepatocyte nuclear factor 6 regulates liver gene expression. Mol. Cell. Biol. *16*, 6273–6284.

Sato, S., Inoue, T., Terada, K., Matsuo, I., Aizawa, S., Tano, Y., Fujikado, T., and Furukawa, T. (2007). Dkk3-Cre BAC transgenic mouse line: a tool for highly efficient gene deletion in retinal progenitor cells. Genesis *45*, 502–507.

Sidman, R. (1961). Histogenesis of the mouse retina studied with thymidine 3-H. In The Structure of the Eye, G.K. Smelser, ed. (New York: Academic Press), pp. 487–506.

Swaroop, A., Kim, D., and Forrest, D. (2010). Transcriptional regulation of photoreceptor development and homeostasis in the mammalian retina. Nat. Rev. Neurosci. *11*, 563–576.

Tian, E., Kimura, C., Takeda, N., Aizawa, S., and Matsuo, I. (2002). Otx2 is required to respond to signals from anterior neural ridge for forebrain specification. Dev. Biol. *242*, 204–223.

Trimarchi, J.M., Stadler, M.B., Roska, B., Billings, N., Sun, B., Bartch, B., and Cepko, C.L. (2007). Molecular heterogeneity of developing retinal ganglion and amacrine cells revealed through single cell gene expression profiling. J. Comp. Neurol. *502*, 1047–1065.

Trimarchi, J.M., Harpavat, S., Billings, N.A., and Cepko, C.L. (2008). Thyroid hormone components are expressed in three sequential waves during development of the chick retina. BMC Dev. Biol. *8*, 101.

Turner, D.L., and Cepko, C.L. (1987). A common progenitor for neurons and glia persists in rat retina late in development. Nature *328*, 131–136.

Turner, D.L., Snyder, E.Y., and Cepko, C.L. (1990). Lineage-independent determination of cell type in the embryonic mouse retina. Neuron *4*, 833–845.

Vandendries, E.R., Johnson, D., and Reinke, R. (1996). orthodenticle is required for photoreceptor cell development in the Drosophila eye. Dev. Biol. *173*, 243–255.

West, E.L., Gonzalez-Cordero, A., Hippert, C., Osakada, F., Martinez-Barbera, J.P., Pearson, R.A., Sowden, J.C., Takahashi, M., and Ali, R.R. (2012). Defining the integration capacity of embryonic stem cell-derived photoreceptor precursors. Stem Cells *30*, 1424–1435.

Wetts, R., and Fraser, S.E. (1988). Multipotent precursors can give rise to all major cell types of the frog retina. Science *239*, 1142–1145.

Wu, F., Sapkota, D., Li, R., and Mu, X. (2012). Onecut 1 and Onecut 2 are potential regulators of mouse retinal development. J. Comp. Neurol. *520*, 952–969.

Yaron, O., Farhy, C., Marquardt, T., Applebury, M., and Ashery-Padan, R. (2006). Notch1 functions to suppress cone-photoreceptor fate specification in the developing mouse retina. Development *133*, 1367–1378.

Yoshida, S., Mears, A.J., Friedman, J.S., Carter, T., He, S., Oh, E., Jing, Y., Farjo, R., Fleury, G., Barlow, C., et al. (2004). Expression profiling of the developing and mature Nrl-/- mouse retina: identification of retinal disease candidates and transcriptional regulatory targets of Nrl. Hum. Mol. Genet. *13*, 1487–1503.

Young, R.W. (1985). Cell differentiation in the retina of the mouse. Anat. Rec. *212*, 199–205.